AUT Journal of Electrical Engineering

AUT J. Elec. Eng., 54(1) (2022) 39-48
DOI: 10.22060/eej.2021.20368.5428

Soft Switched Flyback Converter Using Active Lossless Snubber

Monireh Ghorbanian [1], Hosein Farzanehfard [1*], Morteza Esteki [2]

[1] Department of Electrical and Computer Engineering, Isfahan University of Technology, Isfahan, Iran
[2] Department of Electrical and Computer Engineering University of Alberta, Edmonton, AB, Canada

ABSTRACT: In this paper, a new active lossless snubber circuit is proposed, which provides a soft-switching condition for the traditional Pulse Width Modulation (PWM) fly-back converter. This active lossless snubber circuit creates Zero Voltage Switching (ZVS) condition for the main switch, while Zero Current Switching (ZCS) condition is achieved for the auxiliary switch. Moreover, based on the soft-switching condition, diode reverse recovery problem is omitted and leads to reduction of switching losses and increased efficiency. Additionally, the voltage stress of the auxiliary switch is clamped to the input voltage level which leads to its low capacitive turn ON loss. Furthermore, the presented active lossless snubber circuit provides soft-switching condition independent from load condition. The main and auxiliary switches do not need an isolated gate driver, since their source pins are connected to the input ground. In this manuscript, the different operating modes are explained in detail, and a comprehensive design procedure is presented. Furthermore, loss breakdown for converter elements is offered at full load. The simulation results of the proposed converter using PSPICE software are shown for 155V input, 24 V, 120 W output, and 100 kHz switching frequency to justify the theoretical analysis. The proposed converter has high efficiency of 94.08% at full load.

Review History:

Received: Aug. 04, 2021
Revised: Aug. 31, 2021
Accepted: Sep. 13, 2021
Available Online: Jun. 01, 2022

Keywords:

Fly-back converter
soft switching
active lossless snubber circuit
zero voltage transition
zero voltage switching
zero current switching

1- Introduction

The Fly-back converter has been widely used in low power applications due to its circuit and control simplicity and lower required components (especially switches), compared to other isolated topologies such as bridge converters [1]. However, in the regular fly-back converter, switching losses are caused by the voltage-current overlap at turn ON/OFF instants. Furthermore, in this converter, the stored energy of the leakage inductance discharges in the switch output capacitance at turn OFF instant, which leads to its high voltage stress on the switch [2-4]. Higher power densities are mostly achieved by rising switching frequency as it results in reducing the volume and weight of the converter passive components. However, increasing the switching frequency leads to increment in Electromagnetic interference (EMI) and switching losses [5-8]. Therefore, soft-switching condition of switches and diodes is one suitable solution. So far, several soft-switching methods are introduced [9]. In some of these methods, an auxiliary circuit is added to the converter to make soft-switching state. According to the operation, the auxiliary circuits are divided into three categories.

The first group of auxiliary circuits is called passive lossless snubber, which can create ZVS at turn-off instant for the converter power switch and ZCS condition at turn-on instant [10, 11]. However, capacitive turn ON loss is significant at high frequencies and leads to low efficiency. An active clamp circuit is the second type of auxiliary circuit which consists of only one capacitor and one switch. However, soft switching is lost at light loads in this method [9] and extra circulating current creates high conduction loss. The other group of soft-switching methods is Quasi Resonant Converters (QRCs) in which the frequency related losses are low [12]. However, in these converters, magnetic components and the output filter cannot be efficiently designed due to variable switching frequency. Furthermore, the voltage and current RMS values are high due to their resonant nature. The last group is active lossless snubber. In this type of auxiliary circuit, usually one or more switches are employed and their duty is to activate the auxiliary circuit in switching transition times. Converters with active lossless snubbers providing ZVS for switches are called Zero Voltage Transition (ZVT) converters, and converters with active lossless snubbers providing ZCS for switches are called Zero Current Transition (ZCT) converters [5]. Generally, it is preferred in ZCT converters to use IGBT switches, due to tailing current elimination, and it is more efficient to use MOSFET switches in ZVT converters since switches capacitive turn ON losses is omitted [4, 5]. So far many active snubber circuits have been proposed for fly-back converters [2, 4, 7, 13-17].

The voltage stress on the conventional two switch fly-back converter switches is limited to the input voltage. However, this converter suffers from high turn-off loss of

*Corresponding author's email: hosein@iut.ac.ir

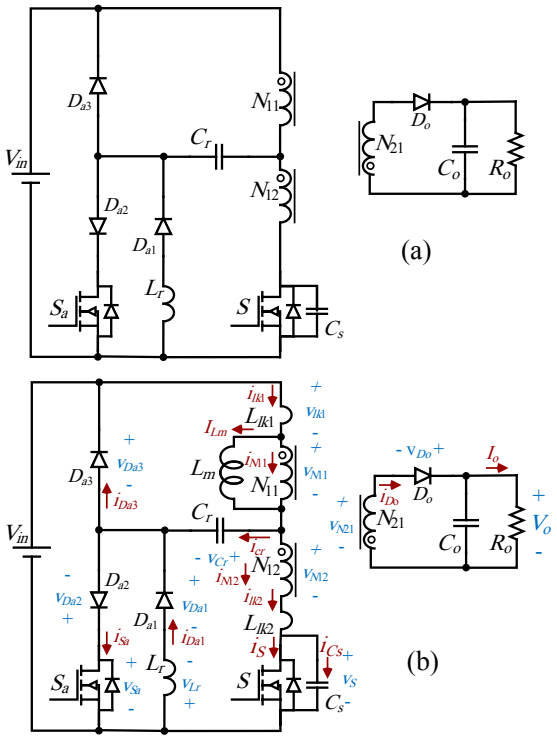

Fig. 1. (a) Proposed converter. (b) Equivalent circuit.

switches. In the active lossless snubbers of [13, 14], the switches can be turned OFF under ZVS condition. However, these converters suffer from high number of elements, high capacitive turn ON loss, and high circulating energy, which lead to low converter power density and efficiency. In [15], a fully soft-switching condition is provided by utilizing an active lossless snubber, while no isolated gate driver is required for both switches as they are connected to the input ground. To transfer the recovered energy to the input source, an extra fly-back type auxiliary transformer is used in this converter. In [4], ZCS condition is achieved for the diodes and the auxiliary switch, and the ZVS condition is provided for the main switch. However, in topology of the active lossless snubber in [4], an additional winding is coupled to the fly-back converter transformer. Therefore, energy circulation is high. Additionally, isolated gate driver is required for the switches and the voltage stress of the switch is higher than the input voltage. In structures [2, 16], no coupled inductors or auxiliary transformer are needed. These active lossless snubbers create ZVS condition for the converter main switch at turn-on instant, while the auxiliary switch operates under ZCS condition for both turn-on and turn-off. Furthermore, in these topologies, isolated gate driver is utilized for the auxiliary switch and its voltage stress is higher than the input voltage level. Two active lossless snubbers are introduced in [7, 17], in which no isolated gate driver or additional transformer is used. However, due to ZCS turn-on of the auxiliary and the high voltage stress of the main switches, switch capacitor turn-on loss in these circuits is considerable. In this research, an improved active auxiliary circuit is proposed to provide ZVS condition for the fly-back converter main switch, while the auxiliary switch operates under ZCS condition. Moreover, the frequent issues in active lossless snubbers namely isolated gate driver, high voltage stress, high element count, and/or auxiliary magnetic components, are eliminated. In section II, the operation principles of the proposed PWM fly-back converter are discussed in detail. In section III, the converter design is explained. In section IV, the simulation results of the fly-back converter are presented to verify the theoretical analysis.

2- Proposed Topology Description

Fig. 1 illustrates the structure of the proposed ZVT fly-back converter. In this topology, V_{in} and V_{out} are the input and the output voltage, S and S_a are the main and the auxiliary switch, C_r and L_r are the resonant capacitor and inductor, C_o and D_o are the output capacitor and the main diode, respectively and C_s is the sum of the snubber capacitor and intrinsic output capacitance of the main switch ($C_s = C_{snubber} + C_{oss}$). The converter transformer is modeled by three ideal windings N_{11}, N_{12} and, N_{21} ($N_{11} = N_{12} = N$ and $N_{21} = 1$), two leakage inductances L_{lk1} and L_{lk2} (

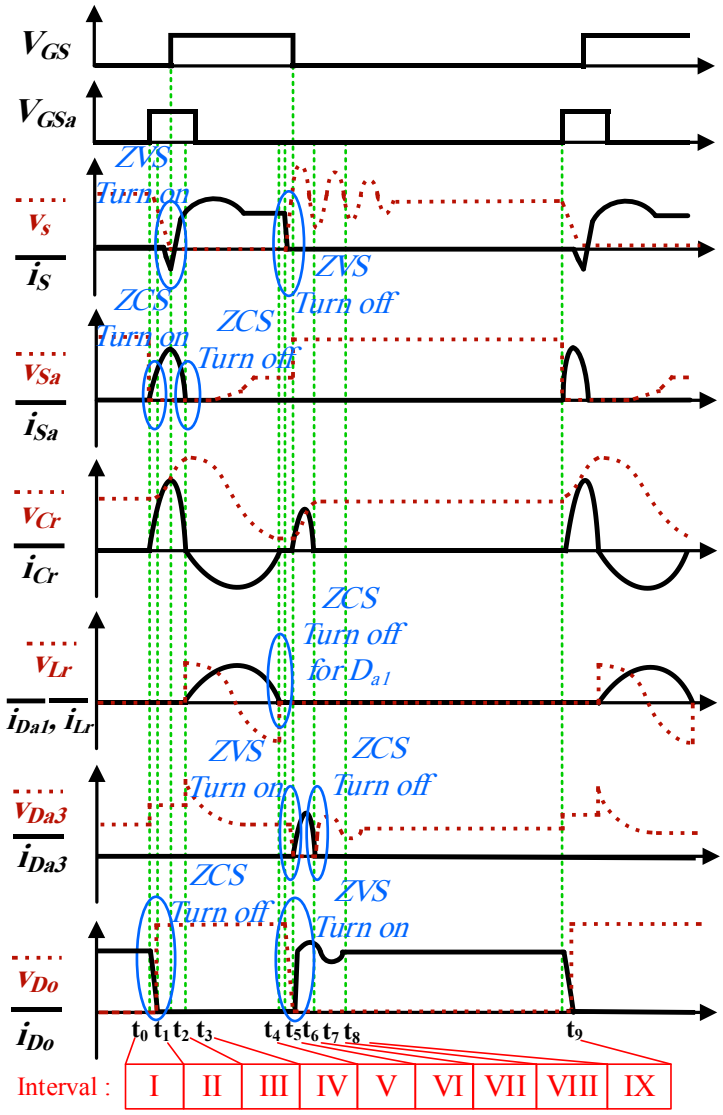

Fig. 2. Theoretical key waveforms of the proposed ZVT fly-back converter.

$L_{lk1} = L_{lk2} = L_{lk}$) and a magnetizing inductance L_m.

3- Operating Principles of the Proposed Converter

The following assumptions are made to simplify the analysis. The proposed converter is in Continuous Condition Mode (CCM), all semiconductor devices are considered ideal, the current passing through the magnetizing inductance ($I_{Lm} = I$), V_{in}, and V_{out} are constant during a switching cycle. The main theoretical waveforms are shown in Fig. 2 and in Fig. 3, nine separate operating modes in one switching period are illustrated.

Interval I $[\mathbf{t}_0, \mathbf{t}_1]$: At t_0, S_a turn-on under ZCS condition. In this mode, two resonant circuits are created consisting of $L_{lk1} - N_{11} - C_r - D_{a2} - S_a - V_{in}$ and $L_{lk2} - N_{12} - C_r - D_{a2} - S_a - C_s$. During this stage, the current of D_o reduces. At the end of this mode, the voltage across C_s reaches V_{in}. Thus:

$$v_{Cr}(t) \approx V_{Cr}(t_0) \tag{1}$$

$$v_S(t) = V_S(t_0) + \big(V_S(t_0) - \tag{2}$$

$$NV_O - V_{Cr}(t_0)\big)\cos[\omega_1(t - t_0)]$$

$$i_{lk2}(t) = \frac{NV_O + V_{Cr}(t_0) - V_S(t_0)}{Z_1}\sin[\omega_1(t - t_0)] \tag{3}$$

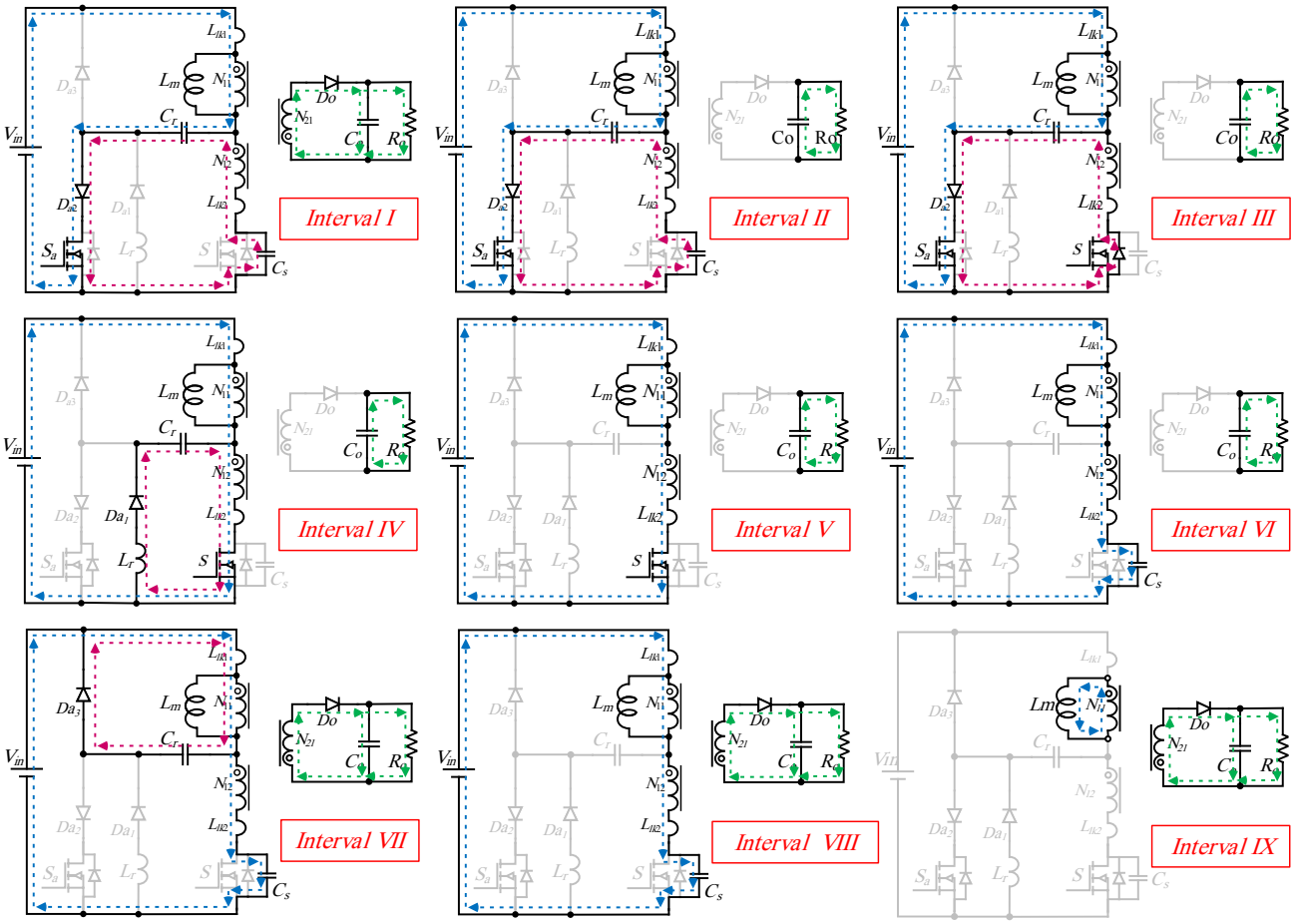

Fig. 3. Equivalent circuits of various operating intervals.

Where:

$$\omega_1 = \frac{1}{\sqrt{L_{lk}C_s}}, Z_1 = \sqrt{\frac{L_{lk}}{C_s}} \tag{4}$$

Interval Ⅱ $[\mathbf{t}_1, \mathbf{t}_2]$: At the end of this mode, the voltage across C_s starts to reduce from V_{in}. Therefore, a negative voltage is placed on the output side and turns the main diode OFF at ZCS state. Similar to the previous interval, two resonances continue until C_s is completely discharged in C_r, and the voltage of C_s reaches zero. Important equations of this interval can be expressed as follows:

$$i_{lk1}(t) = \frac{I.L_{lk}(C_r + 2C_s)}{C_r + 4C_s} + \frac{\frac{1}{2}(V_{in} + V_S(t_1)) - V_{Cr}(t_1)}{Z_2}\sin[\omega_2(t - t_1)] + \left(I_{lk1}(t_1) - \frac{I.L_{lk}(C_r + 2C_s)}{C_r + 4C_s}\right)\cos[\omega_2(t - t_1)] \tag{5}$$

Where:

$$\omega_2 = \frac{1}{\sqrt{L_{lk}C_{eq2}}}, Z_2 = \sqrt{\frac{L_{lk}}{C_{eq2}}}, C_{eq2} = \frac{C_r C_s}{2C_s + \frac{1}{2}C_r} \tag{6}$$

Interval Ⅲ $[\mathbf{t}_2, \mathbf{t}_3]$: At the beginning of this mode, the body diode of S turns ON and the main switch can be turned-on under ZVS state. The resonance continues between $L_{lk1} - N_{11} - C_r - D_{a2} - S_a - V_{in}$, and a new resonance between $C_r - L_{lk2}$ begins. At t_2, S_a, current decreases to zero, and the auxiliary switch can be turned-off under ZCS condition, thus:

$$i_{lk1}(t) = \frac{I}{2} + \frac{\frac{1}{2}V_{in} - V_{Cr}(t_2)}{Z_3}\sin[\omega_3(t - t_2)] + \left(\frac{2I_{lk1}(t_2) - I}{2}\right)\cos[\omega_3(t - t_2)] \tag{7}$$

$$v_{Cr}(t)=V_{Cr}(t_2)+Z_3\left(2I_{lk1}(t_2)-I\right)\sin[\omega_3(t-t_2)]+\left(V_{Cr}(t_2)-\frac{1}{2}V_{in}\right)\cos[\omega_3(t-t_2)] \quad (8)$$

Where:

$$\omega_3=\frac{1}{\sqrt{L_{lk}\frac{C_r}{2}}},Z_3=\sqrt{\frac{L_{lk}}{\frac{C_r}{2}}} \quad (9)$$

Interval Ⅳ $[\mathbf{t}_3,\mathbf{t}_4]$: This mode starts by turning the auxiliary switch OFF at the ZCS state and D_{a2} prevents negative current to flow in S_a. During this mode, C_r is discharging through the resonant circuit of C_r, L_r and L_{lk2}. The important equations of this stage are:

$$I_{Lr}(t_3)=0\Rightarrow i_{Lr}(t)=\frac{V_{Cr}(t_3)-\frac{V_{in}}{2}}{Z_4}\sin[\omega_4(t-t_3)] \quad (10)$$

$$v_{Cr}(t)=V_{Cr}(t_3)+\left(V_{Cr}(t_3)-\frac{V_{in}}{2}\right)\cos[\omega_4(t-t_3)] \quad (11)$$

Where:

$$\omega_4=\frac{1}{\sqrt{L_{eq4}C_r}},Z_4=\sqrt{\frac{L_{eq4}}{C_r}},L_{eq4}=\frac{L_{lk}}{2}+L_r \quad (12)$$

Interval Ⅴ $[\mathbf{t}_4,\mathbf{t}_5]$: In this mode, the introduced converter operation is just like a traditional fly-back converter. This mode finishes when the main switch S is turned-off.

Interval Ⅵ $[\mathbf{t}_5,\mathbf{t}_6]$: At the beginning of this mode, S is turned-off under ZVS condition due to C_s. The current of magnetizing inductance L_m starts to charge C_s until its voltage reaches to $V_{in}+NV_o+v_{cr}+v_{Llk2}$.

Interval Ⅶ $[\mathbf{t}_6,\mathbf{t}_7]$: At t_6, diodes D_{a3} and D_o start conducting. As C_s voltage is greater than V_{in}, a positive voltage is placed on the output side and, D_o is forward biased. The energy of L_{lk1} and L_{lk2} are absorbed by C_r and C_s, respectively. This interval continues until D_{a3} current reaches zero, and C_s voltage becomes equal to its DC voltage level. The related equations of this mode are:

$$v_{Cr}(t)\approx V_{Cr}(t_6) \quad (13)$$

$$i_{lk2}(t)=\frac{V_{in}+V_{Cr}(t_6)+NV_O-V_S(t_6)}{Z_7}\times\sin[\omega_7(t-t_6)]+I_{lk2}(t_6)\cos[\omega_7(t-t_6)] \quad (14)$$

$$v_s(t)=V_s(t_6)-\left(Vin+V_{Cr}(t_6)+NV_O-V_S(t_6)\right)\times\cos\left[\omega_7(t-t_6)\right]+\left(Z_7.I_{lk2}(t_6)\right)\sin\left[\omega_7(t-t_6)\right] \quad (15)$$

Where:

$$\omega_7=\frac{1}{\sqrt{L_{lk}C_s}},Z_7=\sqrt{\frac{L_{lk}}{C_s}} \quad (16)$$

Interval Ⅷ $[\mathbf{t}_7,\mathbf{t}_8]$: At the beginning of this stage, a resonant circuit between the transformer leakage inductances and C_s is formed. This interval ends when L_{lk1} and L_{lk2} currents reach zero.

$$i_{lk2}(t)=\frac{V_{in}+2NV_O-V_S(t_7)}{Z_8}\times\sin[\omega_8(t-t_7)]+I_{lk2}(t_7)\cos[\omega_8(t-t_7)] \quad (17)$$

$$v_s(t)=V_s(t_7)+\left(V_S(t_7)-V_{in}-2NV_O\right)\times\cos\left[\omega_8(t-t_7)\right]+\left(Z_7.I_{lk2}(t_7)\right)\sin\left[\omega_8(t-t_7)\right] \quad (18)$$

Where:

$$\omega_8=\frac{1}{\sqrt{2L_{lk}C_s}},Z_8=\sqrt{\frac{2L_{lk}}{C_s}} \quad (19)$$

Interval IX $[\mathbf{t}_8,\mathbf{t}_9]$: In this interval, the transformer magnetizing inductance energy by transferring the main diode D_o to the output load.

4- Converter Design Consideration

By using the volt-second balance principle on the magnetizing inductance, the introduced converter conversion ratio is attained as follows:

$$\frac{V_o}{V_{in}} = \frac{N_{21}}{N_{11}} \cdot \frac{D}{1-D} \tag{20}$$

Capacitor C_s is obtained similar to the conventional turn-off snubber capacitor [18], as follows:

$$C_S \geq C_{S\min} = \frac{I_S t_f}{2V_S} \tag{21}$$

where I_s is the main switch current before turn-off, t_f is the fall time of the switch current which is found in datasheet and V_s is the main switch voltage after turn-off. When the main switch turns OFF, the main switch current decreases from $\frac{I_o}{\sqrt{8}}$ to zero. Thus:

$$C_{S\min} = \frac{I_O t_f}{2\sqrt{8}V_S} \tag{22}$$

and also:

$$C_{snubber} = C_s - C_{oss} \tag{23}$$

During intervals I and II, the capacitor C_r must completely discharge C_s. Hence, the time duration of these intervals are very short. As the switching period is equal to 10 µs, and the resonance period is considered 0.8 µs. Thus:

$$T_{res} \leq \frac{1}{10} T_{sw} \Rightarrow T_{sw} = 10\mu s \Rightarrow T_{res} = 0.8\mu s \tag{24}$$

$$T_{res} = 2\pi\sqrt{L_{lk2}.C_{eq2}} \Rightarrow 0.8 = 2\pi\sqrt{3C_{eq2}} \Rightarrow C_{eq2} \simeq 5nF \tag{25}$$

from (6) and (22):

$$C_{eq2} = \frac{C_s C_r}{2C_s + \frac{C_r}{2}} \Rightarrow 5 = \frac{3.2 \times C_r}{6.4 + \frac{C_r}{2}} \rightarrow C_r = 46nF \tag{26}$$

The capacitor C_r should be discharged through resonance with resonant inductor L_r during the main switch on time. Therefore, half of this resonance period should be less than the main switch minimum on-time, $D_{min}T_{SW}$. The resonant inductor relation is obtained by:

$$\frac{T_{res}}{2} \leq t_{ON} \Rightarrow \pi\sqrt{L_r C_r} \leq D_{\min} T_{sw} \tag{27}$$

$$2.3\pi\sqrt{L_r C_r} = D_{\min} T_{sw} \Rightarrow L_r = \frac{D_{\min}{}^2 T_{sw}{}^2}{(2.3)^2 \pi^2 C_r} \tag{28}$$

At the beginning of stage VII, the voltage of the snubber capacitor C_s is equal to the sum of the transferred output voltage to the transformer primary side and the input voltage. Afterwards, the stored energy of L_{lk2} starts to discharge in the snubber capacitor C_s and its voltage increases. Therefore, maximum voltage across the main switch can be expressed as:

$$v_{S,\max} = V_{in} + \left(\frac{N_{21}}{N_{11}+N_{12}}\right) V_o + \sqrt{\frac{L_{lk2}}{C_s}} \times i_{N12,\max} \tag{29}$$

Where:

$$i_{N12,\max} = \frac{N_{21}}{N_{12}} I_o \tag{30}$$

The Maximum current of the main switch S happens during mode IV which the resonant capacitor C_r is discharged into the resonant inductor L_r by the main switch. The current stress and the RMS current flowing through the main switch are approximately:

$$i_S = i_{Lr} + i_{lk1} = \frac{1}{2}\left(i_{Lr} + I\right) \tag{31}$$

$$i_{S,\max} = \frac{V_{Cr}(t_3) - \frac{V_{in}}{2}}{2Z_4} + \frac{I}{2} \tag{32}$$

$$I_{S,rms} \approx i_{S,\max}\sqrt{D} \tag{33}$$

The Maximum voltage of the auxiliary switch is clamped to the input voltage level V_{in}, by D_{a3}.

At the end of mode II, the snubber capacitor C_s is completely depleted by C_r through S_a. Based on (5) and

Table 1. Utilized converter components

Component	Specification
Input voltage V_{in} (V)	155
Output voltage V_O (V)	24
Output power P_O (W)	120
Switching frequency f_{sw} (kHz)	100
Duty cycle D	0.38
Switch S	IRFP460
Switch S_a	IXFP80N25X3
Diodes D_{a1}, D_{a2}, D_O	VS-20CTQ150-M3
Diodes D_{a3}	MUR1640
Inductor L_r (µH)	5
Capacitor C_O (µF)	100
Capacitor C_r (nF)	47
Capacitor $C_{snubber}$ (nF)	3.3
Leakage inductances L_{lk1}, L_{lk2} (µH)	3
Turns ratio (N_{11} +N_{12}) / N_{21}	$\sqrt{8}$
Magnetizing inductance L_m (mH)	0.5

(6), the maximum and the RMS current flowing through S_a are expressed by:

$$i_{Sa} = i_{Cr} = 2i_{lk1}(t) - I \tag{34}$$

$$i_{Sa,\max} = \left(\frac{2L_{lk}(C_r + 2C_{st})}{C_r + 4C_{st}} - 1\right) I + 2\sqrt{\left(\frac{\frac{1}{2}(V_{in} + V_S(t_1)) - V_{Cr}(t_1)}{Z_2}\right)^2 + \left(I_{lk1}(t_1) - \frac{I\,L_{lk}(C_r + 2C_s)}{C_r + 4C_s}\right)^2} \tag{35}$$

$$I_{Sa,rms} = i_{Sa,\max}\sqrt{\frac{2\pi}{\omega_2 T_{sw}}} \Rightarrow I_{Sa,rms} = \tag{36}$$

$$i_{Sa,\max}\sqrt{2\pi f_{sw}\sqrt{L_{lk}C_{eq2}}}$$

5- Simulation Result

A 120W prototype converter is designed and simulated by PSPICE software to verify the proposed converter operation and the theoretical analysis. In Table 1, the utilized components and parameters of this converter are illustrated. In Fig. 4, the simulation results of the presented converter are displayed at full load. As can be demonstrated from Fig. 4 (a) and (b), the capacitive turn ON loss of this converter is low. since the main switch turns ON under ZVS condition and the voltage stress of the auxiliary switch is limited to input voltage level. Furthermore, in the introduced converter, soft switching of the auxiliary switch at turn-on and turn-off is under ZCS state while the main switch is under ZVS condition. The current and voltage waveforms of D_{a1}, D_{a3} and D_O are shown in Fig. 4 (c), (d) and (e) respectively. The current waveform

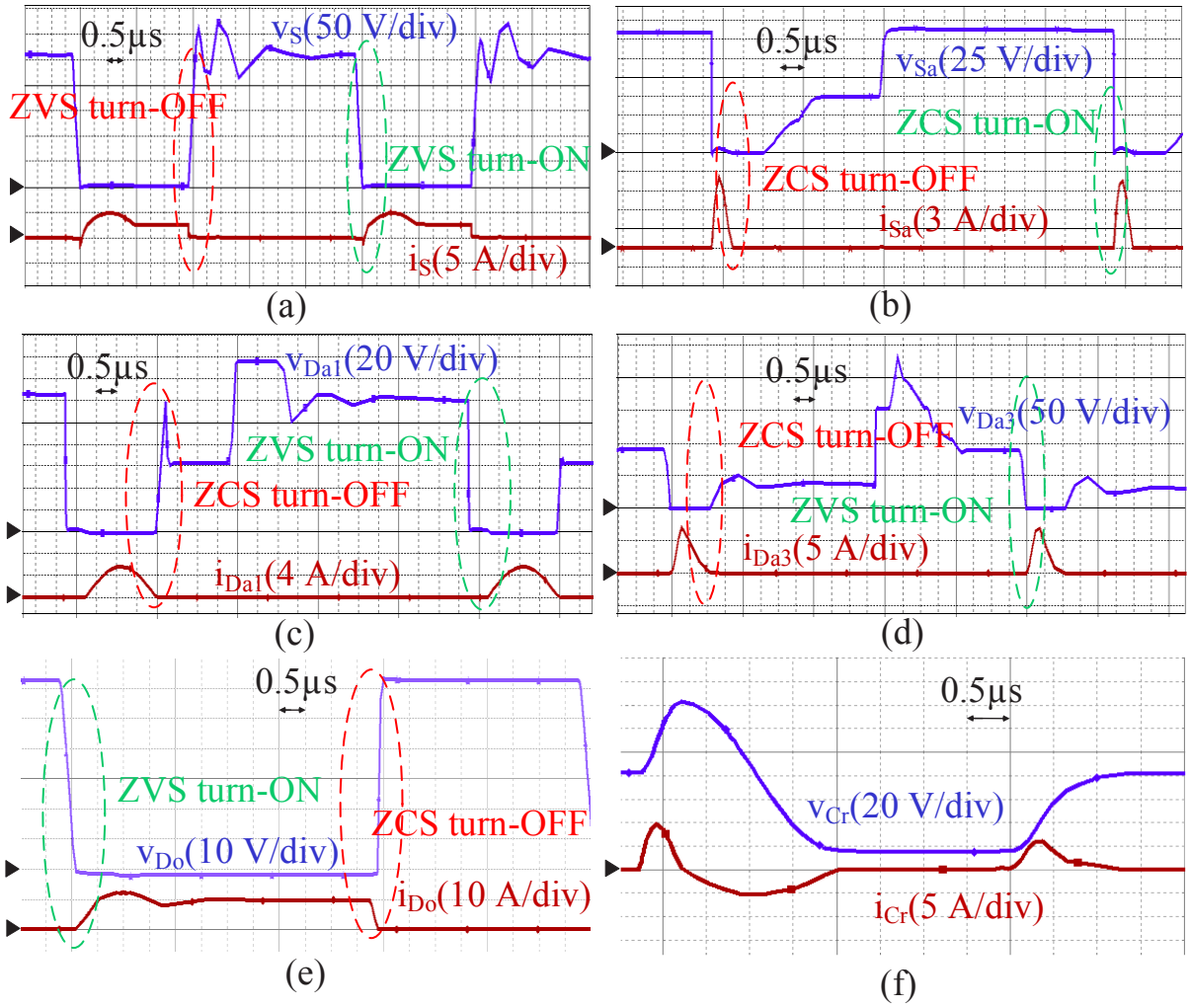

Fig. 4. Voltage and current waveforms of the (a) main switch S (b) auxiliary switch S_a (c) auxiliary diode D_{a1} (d) auxiliary diode D_{a3} (e) output diode D_O and (f) resonant capacitor C_r in the ZVT fly-back converter using PSPICE Software at full load (V_{in}=155 V, P_{out}=120 W).

of diode D_{a2} is similar to the auxiliary switch, as they are in series. According to Fig. 4, all the auxiliary diodes and output diode are turned OFF under ZCS state. As a result, the reverse recovery problem is solved. Moreover, the current and voltage waveform of resonant capacitor is depicted in Fig. 4 (f). In Fig. 5 and Fig. 6, the current and voltage waveforms of the main switch and the auxiliary switch are illustrated at light load and half load, respectively. As can be demonstrated, soft-switching condition is independent of the load. Fig. 7 indicates the simulated loss analysis of the presented converter elements at full load. According to the total power loss, the overall efficiency of 94.08% is obtained for the introduced converter.

6- Conclusions

In this paper, soft-switching condition is created by an active lossless snubber for the PWM fly-back converter. As a result, the voltage-current overlap loss is removed. In fact, the main and the auxiliary switch operate under ZVS conditions and ZCS states, respectively. As a result, the main switch capacitive turn ON loss is eliminated. Furthermore, the capacitive turn ON loss is low in the auxiliary switch, as its voltage stress is much lower than the main the switch voltage. Moreover, all diodes turn OFF under ZCS condition and reverse recovery problem is mitigated. Furthermore, this topology does not require any isolated gate driver.

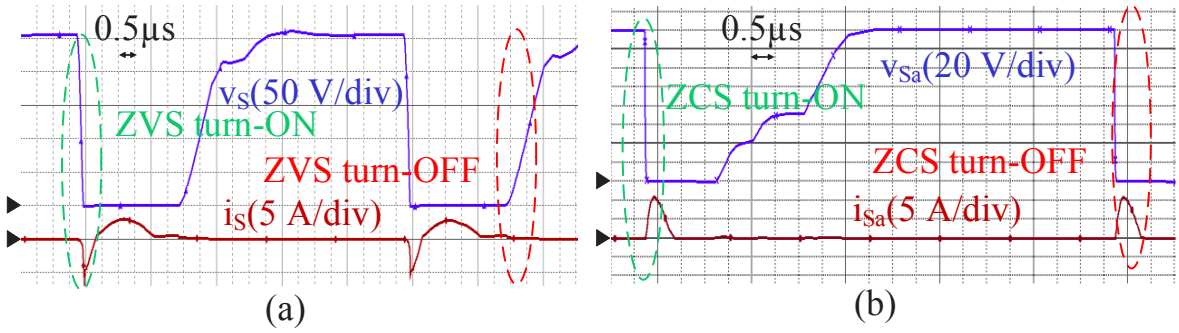

Fig. 5. Voltage and current waveforms of the (a) main switch S (b) auxiliary switch S_a using PSPICE software at light load (V_{in}=155 V, P_{out}=12 W).

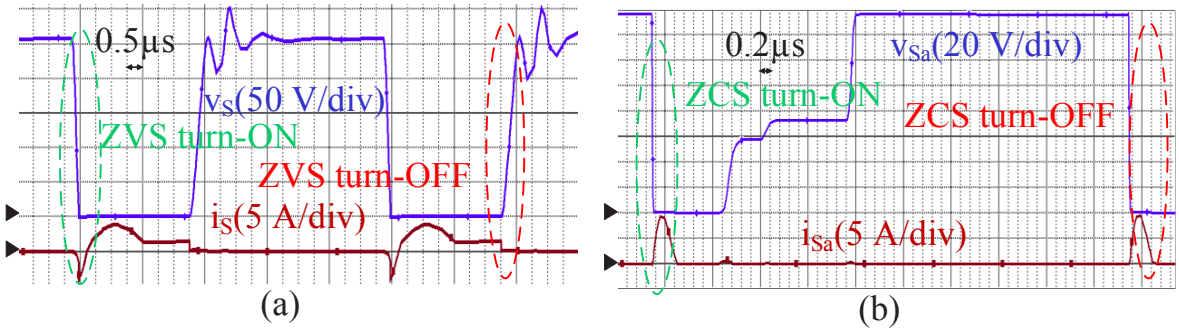

Fig. 6. Voltage and current waveforms of the (a) main switch S (b) auxiliary switch S_a using PSPICE software at half load (V_{in}=155 V, P_{out}=60 W).

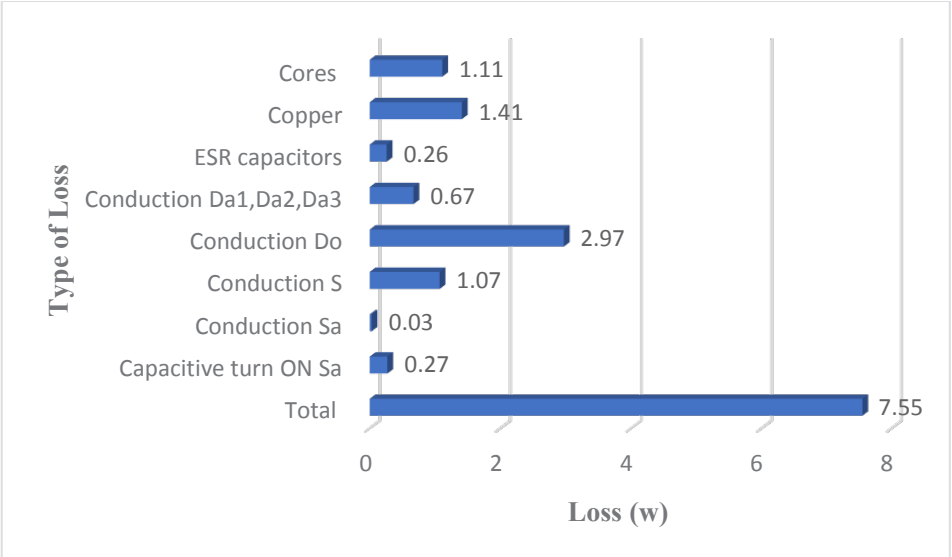

Fig. 7. Loss analysis of the proposed fly-back converter elements using PSPICE software.

References

[1] M. J. Esfandani, M. Feizi, R. Beiranvand, CCM operation of a single stage boost-flyback converter with active-clamp for led driver applications, in: 2020 11th Power Electronics, Drive Systems, and Technologies Conference (PEDSTC), IEEE, (2020), 1-6.

[2] C. Wang, C. Su, C. Yang, ZVS-PWM flyback converter with a simple auxiliary circuit, IEE Proceedings-Electric Power Applications, 153(1) (2006) 116-122.

[3] M. R. Yazdani, S. Rahmani, A new zero-current-transition two-switch flyback converter, in: 2014 5th Power Electronics, Drive Systems, and Technologies Conference (PEDSTC), IEEE, (2014), 390-395.

[4] E. Adib, H. Farzanehfard, New zero voltage switching PWM flyback converter, in: 2010 5th Power Electronics, Drive Systems, and Technologies Conference (PEDSTC), IEEE, (2010), 196-200.

[5] B. Aklaghi, H. Farzanehfard, Family of ZVT interleaved converters with low number of components, IEEE Transactions on Industrial Electronics, 65(11) (2018) 8565-8573.

[6] S. Khalili, N. Molavi, H. Farzanehfard, Soft-switched asymmetric interleaved WCCI high step-down converter with low voltage stress, IEEE Journal of Emerging and Selected Topics in Power Electronics, (2021).

[7] C. Wang, A novel ZCS-PWM flyback converter with a simple ZCS-PWM commutation cell, IEEE Transactions on Industrial Electronics, 55(2) (2008) 749-757.

[8] S. Khalili, H. Farzanehfard, M. Esteki, High step-down DC-DC converter with low voltage stress and wide soft-switching range, IET Power Electronics, 13(14) (2020) 3001-3008.

[9] R. R. Khorasani, E. Adib, H. Farzanehfard, ZVT resonant core reset forward converter with a simple auxiliary circuit, IEEE Transactions on Industrial Electronics, 65(1) (2018) 242-250.

[10] C. Vartak, A. Abramovitz, K. Smedley, Analysis and design of energy regenerative snubber for transformer isolated converters, IEEE Transactions on Power Electronics, 29(11) (2014) 6030-6040.

[11] M. Mohamadi, M. Ordonez, Flyback lossless passive snubber, in 2015 IEEE Energy Conversion Congress and Exposition (ECCE), (2015) 5896-5901.

[12] K. Davoodi, J. Shokr elahi Moghani, S. Salehi Dobakhshari, A high efficient compact 4th order CLCL converter features to use constant current power supply, AUT journal of Electrical Engineering, 51(1) (2019) 63-70.

[13] R. T. H. Li, H. S. Chung, A passive lossless snubber cell with minimum stress and wide soft-switching range, IEEE Transactions on Power Electronics, 25(7) (2010) 1725-1738.

[14] K. Soltanzadeh, M. R. Yousefi, Analysis and design of two-switch flyback converter with double passive lossless snubber, IET Power Electronics, 11(7) (2018) 1187-1194.

[15] Y. Xi, P. Jain, G. Joos, Y. F. Liu, An improved zero voltage switching flyback converter topology, in: PESC 98 Record. 29th Annual IEEE Power Electronics Specialists Conference (Cat. No. 98CH36196), IEEE, (1998) 923-929.

[16] E. Adib, H. Farzanehfard, Family of zero current zero voltage transition PWM converters, IET Power Electronics, 1(2) (2008) 214-223.

[17] CH. M. Wang, J. H. Su, CH. H. Yang, A novel ZCS-PWM flyback converter with a simple ZCS-PWM auxiliary circuit, in: 2005 International Conference on Power Electronics and Drives Systems, (2005) 805-810.

[18] J. G. Kassakian, M. F. Schlecht, G. C. Verghese, Principles of Power Electronics, (2000).

HOW TO CITE THIS ARTICLE

M. Ghorbanian, H. Farzanehfard, M. Esteki, Soft Switched Flyback Converter Using Active Lossless Snubber, AUT J. Elec. Eng., 54(1) (2022) 39-48.

DOI: 10.22060/eej.2021.20368.5428